(Received 18 October 2024, Accepted 31 December 2024, Scheduled 12 January 2025)

Broadband Circularly Polarized Crossed Dipole Antenna Loaded with Magneto-Electric Dipole

Zhuopeng Wang[1], Xin Zhang[2], Haoyu Fang[3], Ao Ni[3], and Yanhui Cheng[1,4,*]

[1] *Taishan College of Science and Technology, Taian, China*
[2] *Jinan Vocational College, Jinan, China*
[3] *Shandong University of Science and Technology, Qingdao, China*
[4] *University Featured Laboratory of Materials Engineering for Agricultural Machinery of Shandong Province, Weifang, China*

ABSTRACT: A right-hand circularly polarized (RHCP) crossed dipole antenna with wide impedance and axial ratio bandwidth is developed. The antenna is composed of a pair of crossed dipoles, four parasitic patches, a metal reflecting cavity, and 12 metal support posts. The four parasitic patches and 12 metal support posts together constitute two pairs of magneto-electric dipoles. By using a quarter wavelength phase delay ring on the crossed dipole, a 90° phase difference between the upper and lower arms is obtained, thereby realizing circularly polarized radiation. By adding slotted parasitic patches, grounded metal posts, and modifying the cavity structure, the circular polarization performance of the antenna is improved. The measurement results show that the antenna with a compact size, low cost obtains 64.5% of impedance bandwidth (1.85–3.61 GHz) and 59.6% of axial ratio bandwidth (1.92–3.55 GHz), and has stable pattern and gain in the operating bandwidth, highlighting significant potential for future applications in sub-6 GHz 5G applications.

1. INTRODUCTION

Many fifth-generation (5G) antennas have been implemented in sub-6 GHz bands [1] and widely used in schools, theaters, stations, airports, and other public places. As the hub is responsible for receiving and sending data in current communication system [2], the antenna has higher requirements, such as circular polarization [3], good bandwidth [4], and efficiency [5]. Among them, circular polarization plays an important role in of 5G wireless standards operating across sub-6 GHz for its self-advantages in reducing polarization mismatch and multipath interference [6]. The basic mechanism of a circularly polarized antenna is to radiate two field components with equal amplitude and orthogonal phases [7]. In the past few years, many circularly polarized antennas with good performance have been studied in [8, 9].

Currently, there are many ways to achieve circular polarization. One way of thinking is to overlay a polarization converter to convert linear polarization into circular polarization [10], while another way of thinking is to directly excite two mutually perpendicular current modes with a phase difference of 90° [11]. A biconical radiating structure [10] surrounded by inner- and outer-circular parallelepiped elements is proposed to convert linearly polarized electric fields into CP fields. This CP antenna exhibits a good gain of 8.5 dBic, but its circular polarization bandwidth can only reach 11.22%. In addition, the patch antenna design [11], which comprises a feeding loop, four L-shaped radiating patches, and a square ground plane, generates orthogonal current distributions on the patch, achieving a good gain of 8.3 dBic, but its circular polarization bandwidth can only reach 5.3%. To achieve broadband CP performance, a butterfly parasitic element is introduced between the two arms of the crossed butterfly dipole to generate additional resonance [12], which significantly broadens the axial ratio (AR) bandwidth of the antenna and achieves 68.9% (1.9–3.9 GHz) impedance bandwidth and 58.6% (2.05–3.75 GHz) AR bandwidth. Similar to crossed dipole, a magneto-electric (ME) dipole was put forward by Luk and Wong in 2006 [21], which achieves 43.8% (1.85–2.89 GHz) wide impedance bandwidth, and obtains stable radiation pattern and gain in the whole bandwidth. Further, an improved circularly polarized magneto-electric dipole antenna [13] was proposed in 2014, which has a 3-dB AR bandwidth of more than 40%. A novel magneto-electric (ME) dipole with a pair of vacant-quarter printed rings and short-end microstrip lines is proposed in [14], which has 54.9% (2.03–3.56 GHz) impedance bandwidth and 43.6% (2.15–3.35 GHz) 3 dB AR bandwidth. A low-profile air gap-free single-board reflectarray antenna has been developed, incorporating an asymmetric dual-polarized ME dipole structure [15]. The antenna achieves an AR bandwidth of 42% and a peak aperture efficiency of 60%. On the whole, ME dipole can greatly enlarge 3-dB AR bandwidth. Currently, researchers have built upon the foundation of ME dipoles, incorporating elements [16–18] to further enhance circular polarization. Combined with the comparison of these circular polarization implementations, it is finally decided to choose crossed dipole as the circular polarization implementation of 5G systems operating sub-6 GHz antenna in this design.

In this paper, a novel broadband circular polarization antenna is proposed, which has low cross polarization, low back radiation, and symmetrical radiation pattern. The antenna generates

* Corresponding author: Yanhui Cheng (chengyanhui@wfust.edu.cn).

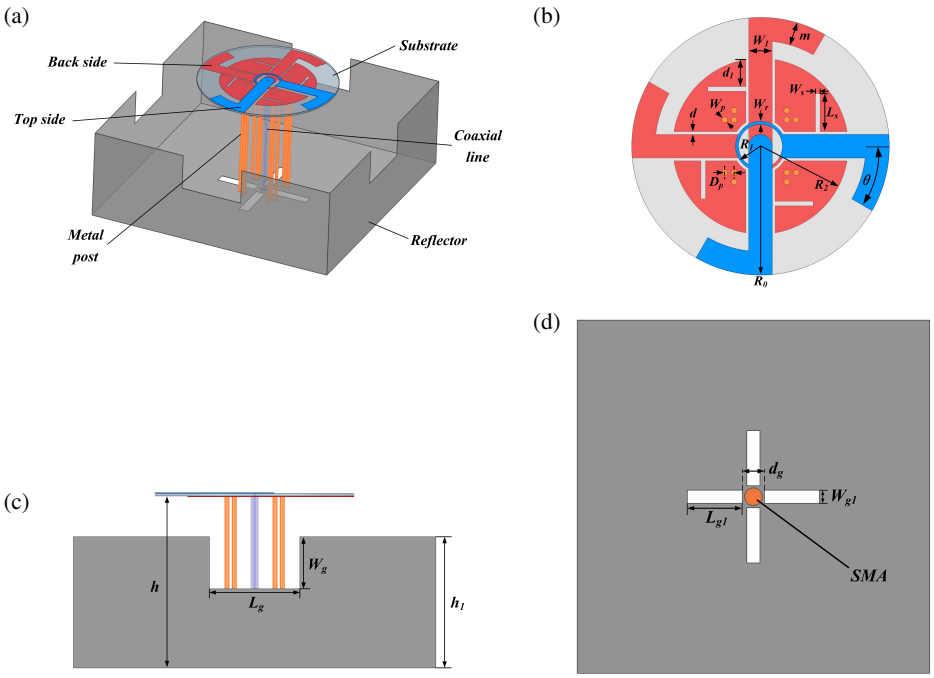

FIGURE 1. Geometry of the proposed antenna. (a) 3D view, (b) top view, (c) side view, (d) bottom view.

a 90° phase difference through a pair of quarter-wavelength phase delay lines and realizes circularly polarized radiation. Two pairs of magneto-electric dipoles are added to produce a stable radiation pattern and gain. The patch in the magneto-electric dipole also serves as the parasitic structure of the crossed dipole, which broadens the axial bandwidth of the antenna. The slotted metal cavity is used as the reflector of the antenna to obtain unidirectional radiation and broaden the antenna AR bandwidth.

2. ANTENNA DESIGN

2.1. Antenna Configuration

The surface currents on two pairs of dipole arms are orthogonal to each other. After each quarter period, the surface current of the antenna is rotated by 90° counterclockwise, resulting in right-handed circularly polarized waves in the direction of the apparent axis. The geometric structure of the antenna is shown in Figure 1. The antenna consists of a crossed dipole loaded with a magneto-electric dipole and a metal reflecting cavity with slots. The overall size of the antenna is $80 \times 80 \times 38\,\text{mm}^3$. The crossed dipole and four parasitic patches are printed on a 0.508 mm-thick Rogers RO4003 substrate with a dielectric constant of 3.55 and a loss tangent of 0.0027. The basic structure of the antenna is a pair of crossed dipoles printed on both sides of a dielectric substrate, and the two arms on the same surface are connected by a quarter-wavelength ring. A square reflecting cavity is added to realize the directional radiation of the antenna. In addition, the circular polarization performance of the antenna is improved by opening a rectangular slot on the wall of the cavity, and the cross polarization of the antenna is reduced by opening a cross slot on the bottom of the cavity. Four sector parasitic patches are added to the bottom of the dielectric substrate to generate additional resonant mode and broaden the bandwidth of the antenna. Three grounded metal posts are welded on each parasitic patch to form two pairs of magneto-electric dipoles. The optimized dimensions of the antenna are listed in Table 1.

TABLE 1. Optimized dimensions of the proposed antenna. **Unit:** mm.

Parameters	Values	Parameters	Values
R_0	22	D_p	1.6
R_1	4	L_s	6.5
R_2	15	W_s	0.8
W_r	0.5	d	0.5
W_p	1	m	4
W_1	4	h	38
h_1	29	L_g	20
W_g	12	L_{g1}	30
W_{g1}	3	d_g	5

2.2. Antenna Mechanism

Figure 2 shows four different antenna evolution models, and Figure 3 depicts the reflection coefficient and AR of the four models to illustrate the antenna design mechanism. Ant. 1 is a circular crossed dipole loaded with a square reflecting cavity, and Ant. 2 is loaded with four sector parasitic patches with strip-shaped slots on the basis of Ant. 1. Compared with Ant. 2, a rectangular slot on the wall of the reflecting cavity and a cross-shaped slot on the cavity bottom are added in Ant. 3. Ant. 4 has three metal posts connected to the ground welded on the bottom surface of each parasitic patch. The impedance band-

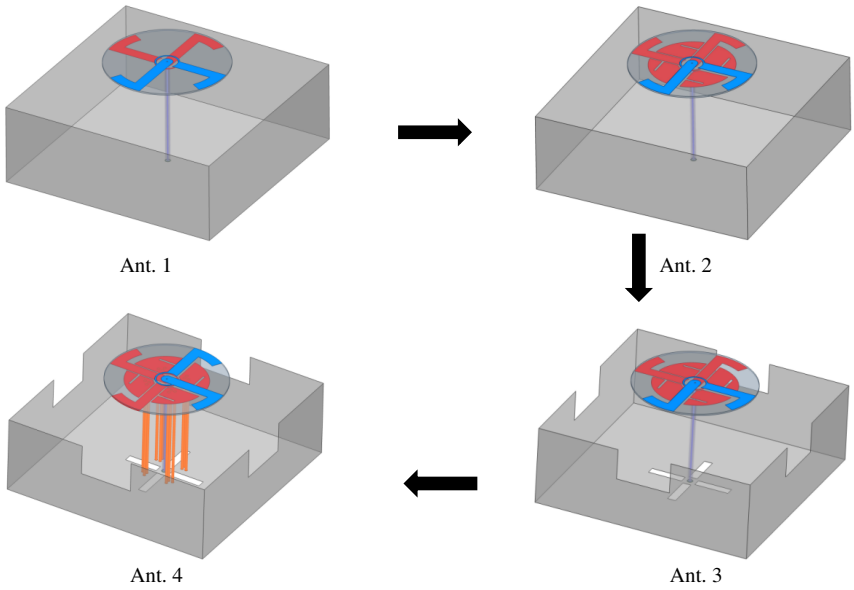

FIGURE 2. Four antenna prototypes in the design process.

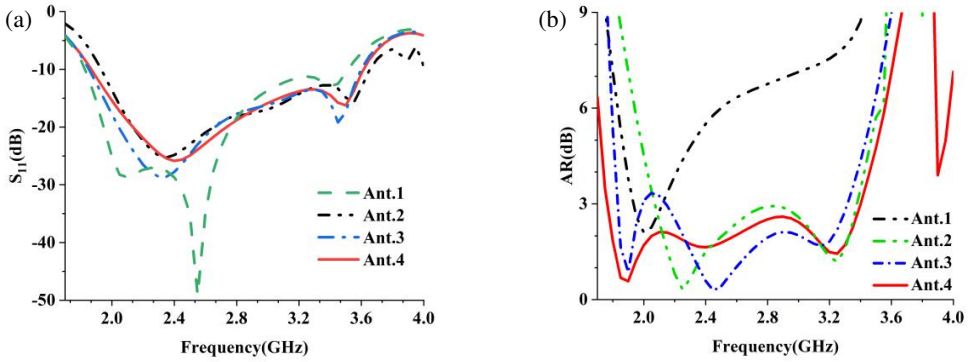

FIGURE 3. Antenna performance. (a) S_{11}, (b) Axial ratio.

width of Ant. 1 is 47% in the range of 1.87–3.02 GHz, and the 3-dB AR bandwidth is only 9.3% in the range of 1.93–2.12 GHz. This is because the antenna only has a circularly polarized resonance mode at 2 GHz. Therefore, four sector parasitic patches are added to Ant. 2 to generate an additional resonance. After adding the parasitic patch, Ant. 2 produces a circularly polarized resonance at 3.25 GHz, and the AR bandwidth is extended to 48%, with a range of 2.07–3.38 GHz. Ant. 3 slots the metal reflector cavity of Ant. 2, resulting in a new circular polarization resonance at 1.9 GHz. However, the AR at 2.05 GHz is still poor, and the broadband circular polarization is not realized. Ant. 4 loads three metal posts connected to the ground on each parasitic patch of Ant. 3. The metal posts and parasitic patch together form a magneto-electric dipole structure, which optimizes the circular polarization radiation of the antenna at low frequency. The 3-dB AR bandwidth reaches 60.4%, and the range is 1.86–3.47 GHz.

The effect of slotted structures on the CP performance is analyzed in Figure 4. It can be seen that the AR bandwidth of the antenna is significantly expanded by the loading of the slot structure. Without the strip slot on the parasitic patch, the antenna only provides 5.2% (2.47–2.61 GHz) and 11.6% (3.15–3.54 GHz) narrow circularly polarized bandwidth respectively. This is because the current of the patch is cut by the slot, so that a new orthogonal current is generated at the edge of the narrow slot; the AR bandwidth is expanded; and the circular polarization performance is improved. The rectangular slot on the wall of the metal cavity also affects the current distribution on the dipole, which extends the axial bandwidth from 43% (2.23–3.45 GHz) to 60.4% (1.86–3.47 GHz).

To explain the principle of circular polarization of the antenna, simulation analysis was performed on the surface current distribution with a period **T** at 3 GHz, as shown in Figure 5. In Figure 5(a), it can be seen that the surface current is mainly concentrated around the gap between the two pairs of dipole arms and the parasitic patch. The surface currents on the two pairs of dipole arms are orthogonal to each other. The surface current rotates 90° counterclockwise every quarter period; therefore a right-handed circularly polarized wave is generated in the boresight direction.

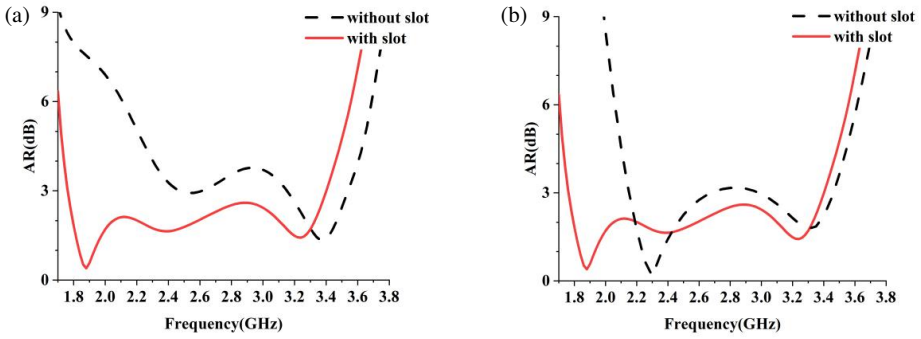

FIGURE 4. Antenna performance with/without slots. (a) Strip slot on the parasitic patch, (b) rectangular slot on the wall of the metal cavity.

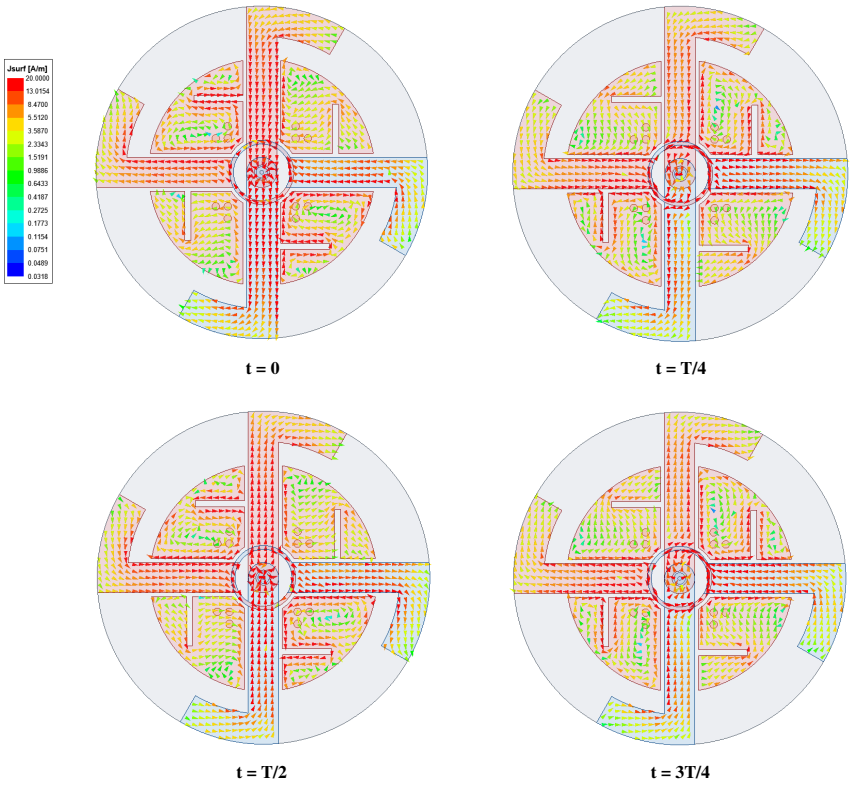

FIGURE 5. Current distributions of the proposed antenna.

2.3. Antenna Parameter Analysis

Several parameters of the antenna are studied to clarify the influence of antenna dimensions on circular polarization performance. Here, the height h of the antenna, the angle θ_1 of the bending part of the crossed dipole, and the distance d between the parasitic patch and crossed dipole are analyzed. The effect of these parameters on the AR is depicted in Figure 6.

In Figure 6(a), it can be observed that when angle θ_1 increases, the dipole arms are effectively elongated, which increases the electrical length of the dipole. This causes the axial ratio bandwidth to shift toward higher frequencies. Additionally, modifications to the bent section of the dipole arms influence the antenna's circular polarization mode, resulting in either a widening or narrowing of the axial ratio bandwidth. The antenna achieves the widest axial ratio bandwidth when θ_1 is set to 32°, making $\theta_1 = 32°$, the optimal configuration.

Figure 6(b) shows the AR varies greatly across the entire bandwidth as the antenna height h changes. As h increases, the circularly polarized resonance moves to low frequency, and the bandwidth is broadened slightly. Therefore, adjusting the antenna profile height is crucial for adjusting the circular polarization effect. Figure 6(c) highlights that the AR bandwidth improves significantly when the distance d is appropriately selected. This is because the gap between parasitic patch and crossed dipole has a significant effect on their coupling, which in turn enhances the AR bandwidth.

3. EXPERIMENTAL RESULTS

For validation, a prototype of the proposed antenna was fabricated and measured. The photographs of fabricated antenna are presented in Figure 7. Figure 8(a) shows the simulated and measured reflection coefficients of the antenna. The sim-

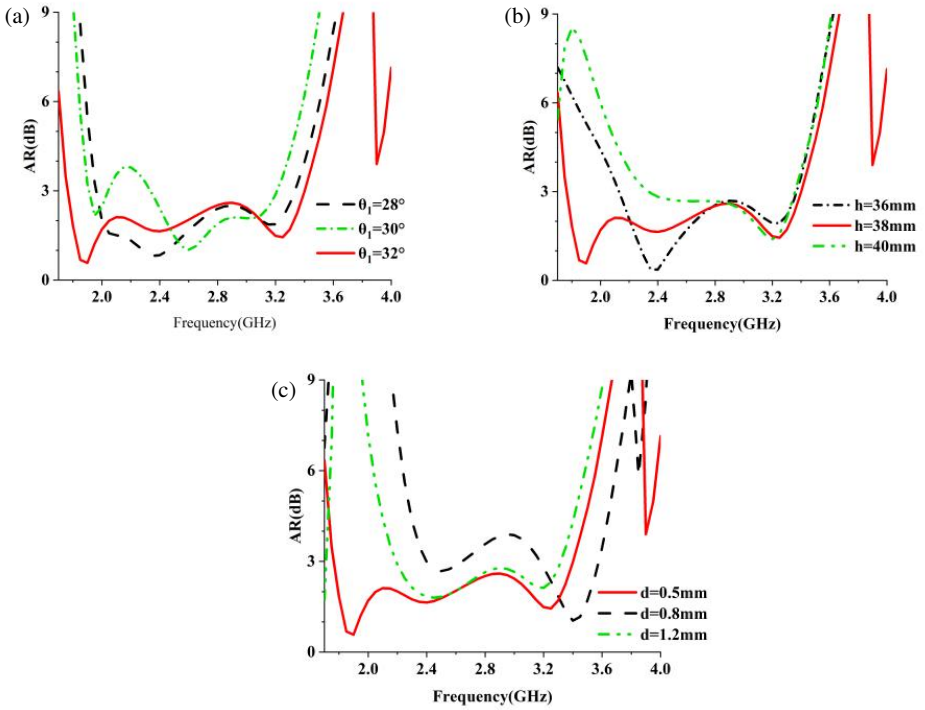

FIGURE 6. Simulated ARs for different parameters: (a) θ_1, (b) h, and (c) d.

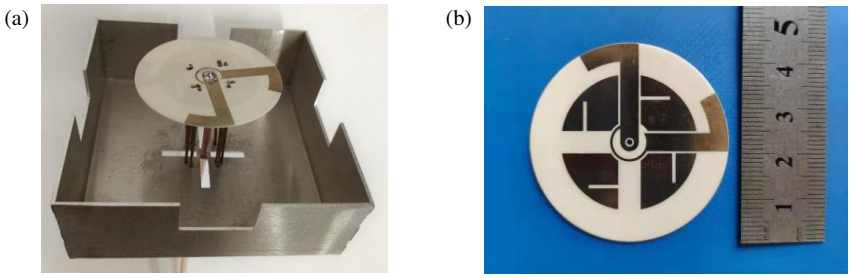

FIGURE 7. Photographs of fabricated antenna. (a) Perspective view, (b) bottom view of the substrate.

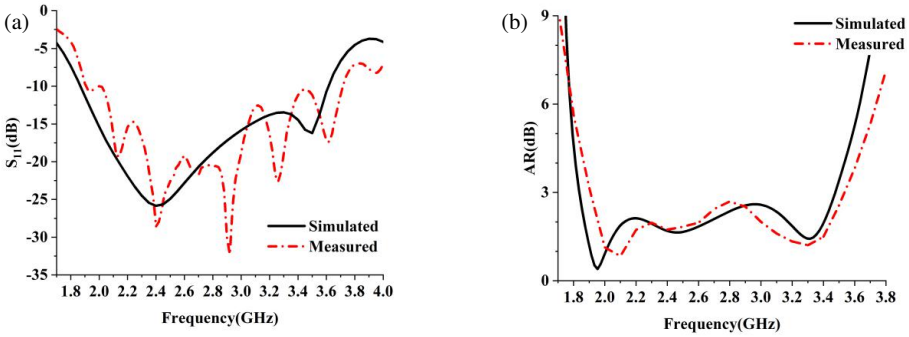

FIGURE 8. Simulated and measured $|S_{11}|$ and ARs of proposed antenna.

ulated and measured impedance bandwidths are 64.5% (1.85–3.61 GHz) and 64.7% (1.89–3.7 GHz), respectively. The simulated and measured ARs are shown in Figure 8(b). It can be observed that the simulated and measured 3-dB AR bandwidths are 60.4% (1.86–3.47 GHz) and 59.6% (1.92–3.55 GHz), respectively. The slight deviation of simulation and measurement results may be caused by fabrication and measurement errors.

Figure 9 depicts the simulated and measured gains of antenna. The measured gain in the entire operation bandwidth is between 6.5 and 8 dBi, which has good stability. Figure 10

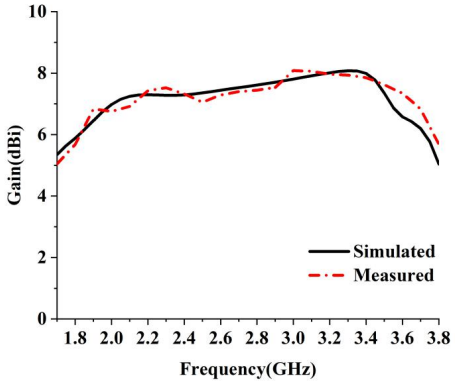

FIGURE 9. Simulated and measured gain of proposed antenna.

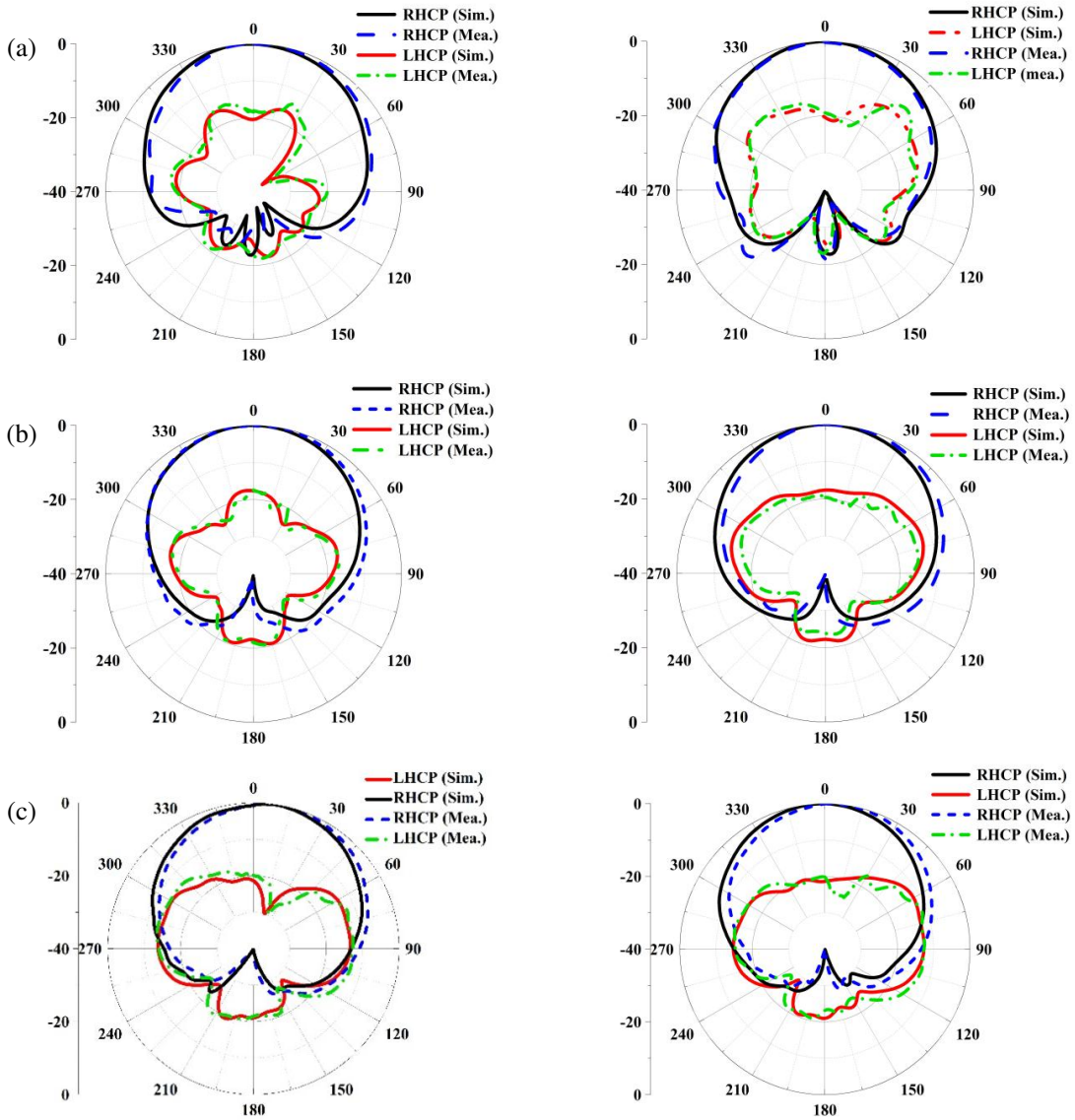

FIGURE 10. Simulated and measured radiation patterns of proposed antenna, (a) 2.3 GHz, (b) 2.7 GHz, (c) 3.2 GHz.

TABLE 2. Comparison of the proposed antenna to previously reported antennas.

Ref. Antenna	Antenna Type	Size (λ_0)	−10 dB IBW (%)	3 dB ARBW (%)	Peak Gain (dBi)
[13]	ME dipole	$1.11 \times 1.11 \times 0.29$	73.3%	47.7%	6.8
[14]	ME dipole	$0.99 \times 0.99 \times 0.18$	54.9%	43.6%	10.3
[15]	ME dipole	$5.96 \times 5.96 \times 0.11$	42%	42%	25.4
[16]	ME dipole + parasitic loop	$1.08 \times 1.08 \times 0.2$	55.3%	42.1%	9.2
[17]	ME dipole + cavity-backed	$0.91 \times 0.91 \times 0.23$	38.73%	33.05%	9.8
[18]	ME dipole + perturbation structure	$6.22 \times 6.22 \times 0.13$	44%	31.5%	20.4
[19]	ME dipole	$4.56 \times 4.56 \times 0.13$	50%	31.7%	22
[20]	ME dipole + AMC	$0.44 \times 0.44 \times 0.1448$	31.6%	23.2%	7.5
Proposed	ME dipole + crossed dipole	$0.69 \times 0.69 \times 0.33$	64.5%	59.6%	8

shows the normalized radiation pattern of the antenna in the XZ ($\varphi = 0°$) and YZ ($\varphi = 90°$) planes at 2.4 GHz and 3.2 GHz. It can be seen that the antenna radiates RHCP waves in the bore-sight direction $(+z)$ and radiates LHCP waves in the opposite direction $(-z)$, and has a symmetrical pattern in the XZ and YZ planes.

Table 2 shows the comparison between the proposed and published circularly polarized cross dipole and magneto-electric dipole antennas, which shows that the antenna has better circularly polarized performance under the same size.

4. CONCLUSION

In this paper, a novel broadband circularly polarized crossed dipole antenna with magneto-electric dipole structure is designed. The antenna consists of a pair of crossed dipoles, a pair of annular quarter wavelength phase delay lines, and two pairs of magneto-electric dipoles. The measurement results show that the antenna has a 10 dB impedance bandwidth of 64.5% (1.85–3.61 GHz) and a 3-dB AR bandwidth of 59.6% (1.92–3.55 GHz). The antenna has the characteristics of compact structure, wide bandwidth, stable gain and radiation pattern in the operation bandwidth. It has potential application value in sub-6 GHz 5G system.

REFERENCES

[1] Jin, G., C. Deng, Y. Xu, J. Yang, and S. Liao, "Differential frequency-reconfigurable antenna based on dipoles for sub-6 GHz 5G and WLAN applications," *IEEE Antennas and Wireless Propagation Letters*, Vol. 19, No. 3, 472–476, Mar. 2020.

[2] Li, S., M. Chen, Z. Li, J. Chen, and J. Wang, "A WLAN dual-polarized beam-reconfigurable antenna," *IEEE Open Journal of Antennas and Propagation*, Vol. 5, No. 4, 869–878, Aug. 2024.

[3] Gao, Y. and W. S. Ji, "Wideband high-gain magneto-electric dipole antenna with novel director loaded," *IEEE Access*, Vol. 12, 117 170–117 175, 2024.

[4] Wang, Z., T. Liang, and Y. Dong, "Compact in-band full duplexing antenna for sub-6 GHz 5G applications," *IEEE Antennas and Wireless Propagation Letters*, Vol. 20, No. 5, 683–687, May 2021.

[5] Zhang, L., K. Wu, S.-W. Wong, Y. He, P. Chu, W. Li, K. X. Wang, and S. Gao, "Wideband high-efficiency circularly polarized SIW-fed S-dipole array for millimeter-wave applications," *IEEE Transactions on Antennas and Propagation*, Vol. 68, No. 3, 2422–2427, 2020.

[6] Hu, Y., Y. M. Pan, and M. D. Yang, "Circularly polarized MIMO dielectric resonator antenna with reduced mutual coupling," *IEEE Transactions on Antennas and Propagation*, Vol. 69, No. 7, 3811–3820, Jul. 2021.

[7] Fakhte, S., H. Oraizi, and R. Karimian, "A novel low-cost circularly polarized rotated stacked dielectric resonator antenna," *IEEE Antennas and Wireless Propagation Letters*, Vol. 13, 722–725, 2014.

[8] So, K. K., H. Wong, K. M. Luk, and C. H. Chan, "Miniaturized circularly polarized patch antenna with low back radiation for gps satellite communications," *IEEE Transactions on Antennas and Propagation*, Vol. 63, No. 12, 5934–5938, 2015.

[9] Sun, J. and K.-M. Luk, "A circularly polarized water patch antenna," *IEEE Antennas and Wireless Propagation Letters*, Vol. 19, No. 6, 926–929, 2020.

[10] Janpangngern, P., D. Torrungrueng, M. Krairiksh, and C. Phongcharoenpanich, "Dual-band circularly polarized omni-directional biconical antenna with double-circular parallelepiped elements for WLAN applications," *IEEE Access*, Vol. 10, 31 970–31 980, 2022.

[11] Yang, W.-J., Y.-M. Pan, and X.-Y. Zhang, "A single-layer low-profile circularly polarized filtering patch antenna," *IEEE Antennas and Wireless Propagation Letters*, Vol. 20, No. 4, 602–606, Apr. 2021.

[12] Tran, H. H., I. Park, and T. K. Nguyen, "Circularly polarized bandwidth-enhanced crossed dipole antenna with a simple single parasitic element," *IEEE Antennas and Wireless Propagation Letters*, Vol. 16, 1776–1779, 2017.

[13] Li, M. and K.-M. Luk, "A wideband circularly polarized antenna for microwave and millimeter-wave applications," *IEEE Transactions on Antennas and Propagation*, Vol. 62, No. 4, 1872–1879, 2014.

[14] Shang, Y., J. Sun, C. Zhou, H. Li, D. Wu, and Q. Zeng, "A broadband circularly polarized magneto-electric dipole antenna," *IEEE Antennas and Wireless Propagation Letters*, Vol. 22, No. 8, 1982–1986, Aug. 2023.

[15] Wu, F., J. Wang, Y. Zhang, W. Hong, and K.-M. Luk, "A broadband circularly polarized reflectarray with magneto-electric dipole elements," *IEEE Transactions on Antennas and Propagation*, Vol. 69, No. 10, 7005–7010, Oct. 2021.

[16] Ding, K., Y. Li, and Y. Wu, "Broadband circularly polarized magnetoelectric dipole antenna by loading parasitic loop," *IEEE Transactions on Antennas and Propagation*, Vol. 70, No. 11, 11 085–11 090, Nov. 2022.

[17] Boontamchauy, P., M. Sano, R. Kuse, and T. Fukusako, "Circularly polarized cavity-backed antenna with variable magneto-electric crossed-dipole structure," *IEICE Communications Express*, Vol. 13, No. 11, 421–425, Nov. 2024.

[18] Wu, F., R. Lu, J. Wang, Z. H. Jiang, W. Hong, and K.-M. Luk, "Circularly polarized one-bit reconfigurable ME-dipole reflectarray at X-band," *IEEE Antennas and Wireless Propagation Letters*, Vol. 21, No. 3, 496–500, Mar. 2022.

[19] Tan, Q., K. Fan, W. Yu, W. Wang, L. Liu, and G. Q. Luo, "A circularly polarized magneto-electric dipole antenna array with wide AR and impedance bandwidth for millimeter-wave applications," *IEEE Antennas and Wireless Propagation Letters*, Vol. 22, No. 9, 2250–2254, Sep. 2023.

[20] Chen, Q., H. Zhang, L.-C. Yang, and T. Zhong, "A metasurface-based slit-loaded wideband circularly polarized crossed dipole antenna," *International Journal of RF and Microwave Computer-Aided Engineering*, Vol. 28, No. 1, e21173, 2018.

[21] Luk, K. M. and H. Wong, "A new wideband unidirectional antenna element," *International Journal of Microwave and Optical Technology*, Vol. 1, No. 1, 35–43, 2006.